Astronomy & Astrophysics manuscript no. LLRD
December 4, 2025

Radio Detection of a Local Little Red Dot

L. F. Rodriguez[1,2] and I. F. Mirabel[3,4]

[1] Instituto de Radioastronomía y Astrofísica, Universidad Nacional Autónoma de México, Apdo. Postal 3-72, Morelia, Michoacán 58089, México
e-mail: l.rodriguez@irya.unam.mx
[2] Mesoamerican Center for Theoretical Physics, Universidad Autónoma de Chiapas, Tuxtla Gutiérrez, Chiapas 29050, México
[3] Département dAstrophysique-IRFU-CEA Université Paris-Saclay, France
[4] Instituto de Astronomía y Física del Espacio (IAFE) CONICET-Universidad de Buenos Aires, C1428 Buenos Aires, Argentina

Received November 29, 2025

ABSTRACT

Context. One of the most important discoveries by the James Webb Space Telescope (JWST) is the unexpected existence in the Early Universe (z > 4) of very large quantities of Little Red Dots (LRDs), compact luminous red galaxies of intriguing physical properties.
Aims. We wish to know if LRDs may host accreting Intermediate/Supermassive Black Holes (IMBHs/SMBHs) that may power LRDs, and compare them with the effect of clusters of massive stars. The spectrum of radio emission (synchrotron vs thermal) can be used to know which between these two types of energy sources is the dominant one.
Methods. So far LRDs at high redshifts have not been detected at radio wavelengths and it is not known why. Assuming this could be due to their large distances and/or present limitations of observational capabilities, we analyze here archive Very Large Array radio observations of two analog candidates of LRDs in the Local Universe (LLRDs) at redshifts z = 0.1 - 0.2.
Results. The LLRD source J1047+0739 at z = 0.1682 is detected at 6.0 GHz in 2018 with the VLA-A of NRAO as a compact source with radii less than 0.2 arc sec (< 600 pc at d = 700 Mpc). Its flux density was 117±8 μJy and its spectral index was -0.85, which is typical of optically-thin synchrotron emission. It is also detected at 5.0 GHz in 2010 with the VLA-C, showing a flux density of 43±3 μJy.
Conclusions. The observed flux densities can be provided by a radio luminous supernova. The increase in flux density over eight years can be explained as the result of two independent supernovae or as the radio re-brightening of a single one. Radio time monitoring of this and other LLRDs could help clarify the mystery of the radio silence of its cosmological counterparts.

Key words. Galaxies: quasars: supermassive black holes – Radiation mechanisms: non-thermal – Radio continuum: galaxies

1. Introduction

Abundant populations of LRDs at z > 4 have been unexpectedly discovered in several JWST surveys in the last two years (e.g., Matthee et al. 2024). LRDs are mostly observed between redshifts of z = 4 and z = 8 with maximum peak density at z = 5, and an exponential decline in numbers at redshifts z < 4 (e.g., Billand et al. 2025), which implies that Local Little Red Dot (LLRD) candidates are scarce in the Local Universe.

LRDs in the Early Universe are extremely compact galaxies with average effective radius of less than a few hundred pc, widths of broad emission lines of up to 2000 km s^{-1}, and V-shaped Spectral Energy Distributions, intrinsically red rather than dust-reddened. These properties together are uncommon in previously known galaxies before JWST. LRDs are not detected or are very dim soft X-ray emitters of less than 10 keV, and have not been detected at radio wavelengths. These physical properties are puzzling, and to explain the dominant energy source of the high luminosities there were proposed two basic kinds of models; one based on highly accreting IMBH/SMBHs, and another based on rich clusters of very massive stars. These latter models have been challenged because of the extreme stellar masses that would be required to produce the high luminosity of LRDs in volumes with radii of only a few hundred pc (Pacucci et al. 2023). On the other hand, the absence of soft X-ray detections in LRDs challenged the accreting IMBH/SMBH models. However, this absence of X-rays has been explained by cold gas absorption in a BH atmosphere with gas densities $n_H > 10^9\ cm^{-3}$, column densities $N_H > 10^{24} cm^{-2}$, and gas turbulent velocities of ∼500 km s^{-1} (e.g., Maiolino, Risaliti, Signorini et al. 2025). Other models models attempted to explain the absence of X-rays and radio emission by free-free absorption, synchrotron self-absorption, and disruption of magnetic field and X-ray corona by super-Eddington accretion (Mazzolari, Gilli, Maiolino, et al. 2024).

Contrary to soft X-rays, radio jet emission may not be totally or even partially absorbed by column densities of $N_H > 10^{24}\ cm^{-2}$. In fact, radio jets are observed from mass accreting stellar BHs while the soft X-rays are completely obscured (e.g., Rodriguez and Mirabel 2025). In addition, we have shown that under the assumption that radio jets are perpendicular to the inner BH accretion disks, radio jets can provide crucial information on the physics of accretion in the inner obscured disks. However, LRDs in the Early Universe so far have been radio silent due to unknown reasons (e.g., Mazzolari et al. 2024; Perger et al. 2025; Akinsăet ală2025; Latif et al. 2025). In this context, the study of LLRDs analogs may help to understand why LRDs at high redshifts are radio silent, and eventually lead in the future to strategies that may result in radio detections of LRDs in the Early Universe.

An immediate possibility to test directly between the competing hypotheses is the analysis of archived radio observations of LLRDs candidates. Two LLRD candidates (SDSS J1025+1402 and SDSS J1047+0739), were serendipitously identified for the first time in the Sloan Digital Sky Survey (SDSS) by Izotov & Thuan (2008). These authors called them Metal Poor Dwarf Emission-Line Galaxies finding in these galaxies signals of an intermediate-mass AGN. It was found that these compact dwarf galaxies had extraordinarily velocity broadened Hα emission with luminosities ranging from 3×10^{41} to 2×10^{42} erg s^{-1}. Their metallicity is very low and the extraordinarily high broad Hα luminosities remained constant over periods of 3-7 yr, which probably excluded Type IIn supernovae as a mechanism for the emission with broad velocities. Further studies on this type of galaxies were made by Simmonds, Bauer, Thuan et al. (2016).

More recently, Xiaojing Lin et al. (2025) showed that those two LLRDs exhibit properties fully consistent with those of high-redshift LRDs. From new Chandra observations they found that these LRDs are very weak in X-rays, and quote several attempts of radio observations that resulted in no detections.

In section 2 the observations are described and the results presented, while in section 3 we interpret the data and summarize our conclusions.

2. Observations

Previous studies of these regions failed to detect radio continuum emission (Burke et al. 2021). We searched for observations of these two LLRDs in the archives of the Very Large Array of NRAO[1]. We found data in two projects: 10B-156 (PI: C. Henkel) and 18A-413 (PI: F. Bauer). The data were analyzed in the standard manner using the CASA (Common Astronomy Software Applications; McMullin et al. 2007) package of NRAO and the pipeline provided for VLA[2] observations. We made images using a robust weighting (Briggs 1995) of 0 to optimize the compromise between angular resolution and sensitivity. All images were also corrected for the primary beam response.

In project 10B-156 both sources were observed. The array was in its C configuration. J1047+0739 was observed at epoch 2010 Nov 06 and J1025+1402 was observed at epoch 2010 Oct 25. In both epochs 0521+166=3C138 was the amplitude calibrator. The gain calibrators were J1007+1356 for J1025+1402 and J1058+0133 for J1047+0739. The bootstrapped flux densities of J1007+1356 and J1058+0133 were 0.971±0.003 and 0.996±0.001 Jy, respectively.

2.1. LLRD J1047+0739

The LLRD J1047+0739 was clearly detected in this first epoch (Figure 1; top) with a flux density of 43±3 μJy. Other parameters of the observations of this source are listed in Table 1.

The data of project 18A-413 were taken with the array in its highest angular resolution A configuration. Only J1047+0739 was observed, on epoch 2018 Apr 20. The amplitude calibrator was 1331+305=3C286 and the gain calibrator was J1058+0133, with a bootstrapped flux density of 6.379±0.024 Jy. Again, the source was clearly detected (Figure 1; bottom), with a flux density of 117±8 μJy. These data were taken with the broad band correlator (with a total bandwidth of 4.0 GHz) and an in-band spectral index determination was possible. For this we divided the spectral windows in four sub-bands 1 GHz wide each and determined the flux densities shown in Figure 2. A least-squares fit to these flux densities gives

$$log[S_\nu(\mu Jy)] = (2.74 \pm 0.18) - (0.85 \pm 0.24)\ log[\nu(GHz)].$$

2.2. LLRD J1025+1402

On the other hand, no source was detected directly associated with J1025+1402. However, about 2 arcsec to its east there is a source detected at a 4-σ level with a flux density of 57±14 μJy (Figure 3). Following the formulation of Anglada et al. (1998) the *a priori* probability of detecting a source with this flux density at the frequency of 5.0 GHz in a solid angle of 4 arcsec^2 is only 0.0004, so the association of the radio source with J1025+1402 seems to be significant. The radio source is unresolved at a scale of 0.″9 (< 1700 pc at d = 420 Mpc). We speculate that the radio emission may be produced in a compact jet emanating from an IMBH/SMBH, and will pursue the study of this source in the future.

3. Discussion and Conclusions

The spectral index of −0.85 is typical of optically-thin synchrotron emission and favors a non-thermal mechanism to produce the radio emission and possibly energize the LRDs. The radio source is unresolved at a scale of 0.″2 (< 600 pc at d = 700 Mpc).

Another important result is the evidence of significant time variability in the radio emission. Correcting the 5.0 GHz flux density of 2010 by a factor $(5.0/6.0)^{-0.85}$ to compare with the 2018 flux density at 6.0 GHz, we find that the flux density has increased by a factor of 2.3±0.2 over this 7.5 yr time period. A detectable variability over a timescale of years is not uncommon in AGNs and again points to a SMBH, but as we will see, another explanation is favored. This important change in radio flux density contrasts with the lack of variability at r-band reported for J1047+0739 at the 3-4% level by Burke et al. (2025).

3.1. Can a Supernova Account for the Radio Emission Observed in J1047+0739?

Can the radio emission detected in LLRD J1047+0739 be explained by a supernova? The most radio luminous supernovae reach values of $L_R \sim 10^{39}$ erg s^{-1} (Kulkarni et al. 1998; Yao et al. 2022). The radio luminosity associated with LLRD J1047+0739 between the rest frequencies ν_2 and ν_1 is given by:

$$L_R = 4\pi D_L^2 S_\nu (1+z)^{1-\alpha} \nu^{-\alpha} (\nu_2^{\alpha+1} - \nu_2^{\alpha+1})/(\alpha+1).$$

We assume that ν_2 = 10 GHz and ν_1 = 1 GHz. We have an observed flux density of S_ν = 0.117 mJy at ν = 6.0 GHz. For z = 0.1682, D_L = 815 Mpc and α = -0.85 we obtain $S_L = 1.6 \times 10^{39}$ erg s^{-1}, a value comparable to that of the most luminous radio supernovae known. We then conclude that the radio emission observed from LLRD J1047+0739 can be explained in terms of a luminous supernova.

It is interesting that the flux density *increases* from 2010 to 2018. This could be explained in terms of two independent supernovae remnants. In this case the supernova rate in

[1] The National Radio Astronomy Observatory is a facility of the National Science Foundation operated under cooperative agreement by Associated Universities, Inc.

[2] https://science.nrao.edu/facilities/vla/data-processing/pipeline

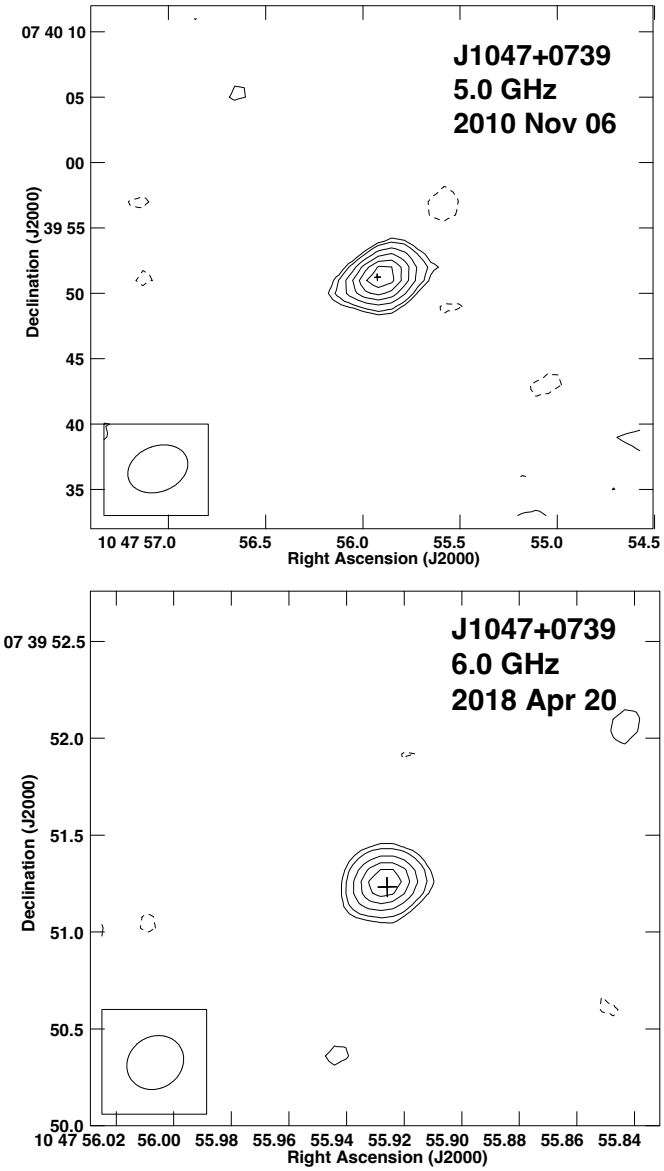

Fig. 1: (Top) VLA contour image of the J1047+0739 region from project 10B-156. Contours are -3, 3, 4, 6, 8, 10 and 12 times 2.6 μJy beam^{-1}, the rms noise in this region of the image. The synthesized beam ($4\farcs7 \times 3\farcs5$; $-69°$) is shown in the bottom left corner. (Bottom) VLA contour image of the J1047+0739 region from project 18A-413. Contours are -3, 3, 4, 6, 8 and 10 times 8.0 μJy beam^{-1}, the rms noise in this region of the image. The synthesized beam ($0\farcs30 \times 0\farcs27$; $-56°$) is shown in the bottom left corner. In both images the cross marks the optical position of the source from the Gaia Early Data Release 3 (Gaia Collaboration 2020).

J1047+0739 would be enormous. However, a single supernova could also account for the observations. It is well known that supernova can suffer radio re-brightening as the ejecta interacts with surrounding gas even years or decades after the explosion (Balasubramanian et al. 2021; Rose et al. 2024; Soria et al. 2025). Monitoring of the radio emission will help understand if J1047+0739 has a high rate of supernovae or if we are observing a single source. As a comparison, the starburst galaxy M82 is estimated to have a supernova rate of ~0.1 yr^{-1} (one every ten years) occurring over a region with ~500 pc in diameter (Strickland 2004; Bolatto et al. 2024).

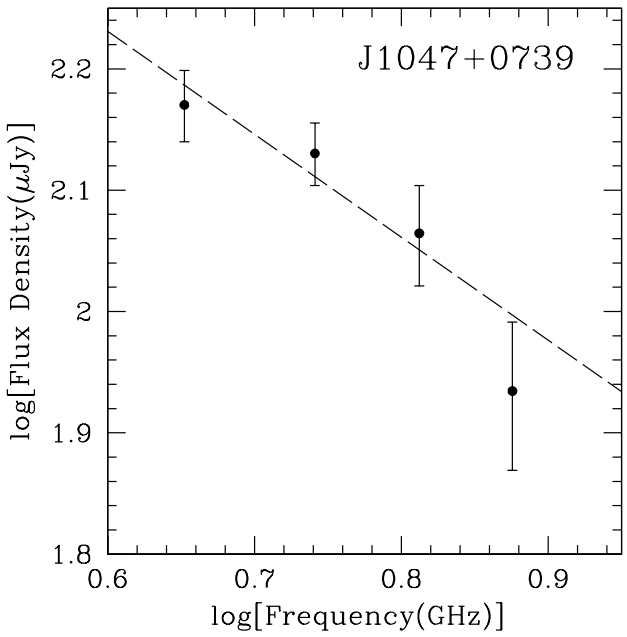

Fig. 2: Flux density as a function of frequency for J1047+0739 from the data of project 18A-413. The least squares fit gives log[S$_\nu$(μJy)] = (2.74±0.18) -(0.85±0.24) log[ν(GHz)]. The spectral index of -0.85 is typical of optically-thin synchrotron emission.

3.2. Expected Radio Flux Density at Cosmological Distances

We can use the measured flux density of LLRD J1047+0739 to predict the flux density expected for an identical source located at cosmological distances. For a radio source with a power-law spectrum given by $S_\nu \propto \nu^\alpha$ the flux density measured at the same frequency and different z values is given by:

$$\left[\frac{S_\nu(z_1)}{S_\nu(z_0)}\right] = \left[\frac{1+z_0}{1+z_1}\right]^{1-\alpha} \left[\frac{D_L(z_0)}{D_L(z_1)}\right]^2,$$

where z is the redshift, S_ν is the flux density, and D_L is the luminosity distance. In our case the reference is LLRD J1047+0739, for which z_0 = 0.1682, D_L = 815 Mpc and α = -0.85. We will derive the expected flux density for a source located at z = 5, the value at which the density of LRDs peaks. For this z we have D_L = 47648 Mpc. We then obtain

$$S_\nu(z=5) = 2.8 \times 10^{-6}\ S_\nu(z=0.1682).$$

The expected flux densities in the centimeter range are very small, of order 1 nJy (nano Jansky) and below the sensitivity of even the next generation of radio interferometers.

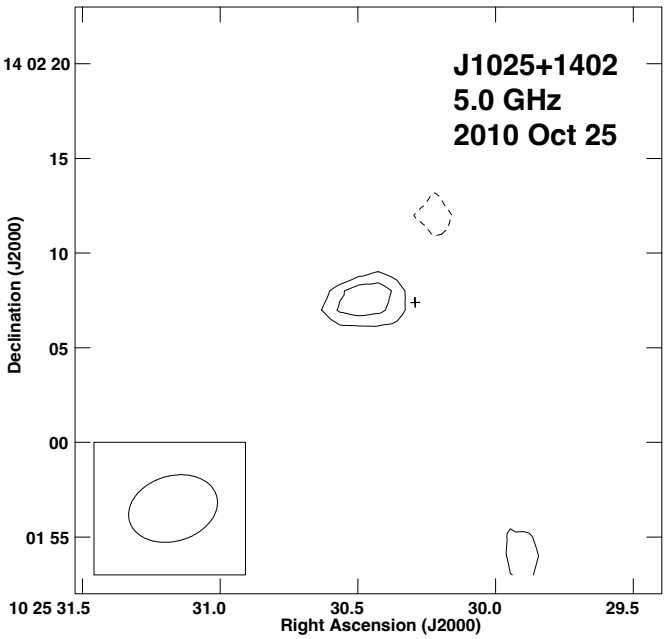

Fig. 3: VLA contour image of the J1025+1402 region from project 10B-156. Contours are -3, 3 and 4 times 14.0 μJy beam^{-1}, the rms in this region of the image. The synthesized beam ($4\farcs8 \times 3\farcs4; -73°$) is shown in the bottom left corner. The cross marks the optical position of the source from the Gaia Early Data Release 3 (Gaia Collaboration 2020).

3.3. Conclusions

We present archive VLA observations that detect radio emission from the LLRD J1047+0739 in two epochs. The radio emission can be understood in terms of a radio luminous supernova. The increase in time of the flux density suggests either two independent supernovae or a single supernova remnant with a radio rebrightening. If the radio emission from cosmological LRDs is limited to that produced by similar supernovae it will be very difficult to detect them in the radio at cm-meter wavelengths, even with the next generation of interferometers.

Acknowledgements. LFR acknowledges support from grant CBF-2025-I-2471 of SECIHTI, Mexico. IFM acknowledges support from DAP-CEA-Saclay for allowing the use of software facilities and institutional access to non-open access publications.

References

Akins, H. B., Casey, C. M., Lambrides, E., et al. 2025, ApJ, 991, 1, 37. doi:10.3847/1538-4357/ade984
Anglada, G., Villuendas, E., Estalella, R., et al. 1998, AJ, 116, 6, 2953. doi:10.1086/300637
Balasubramanian, A., Corsi, A., Polisensky, E., et al. 2021, ApJ, 923, 1, 32. doi:10.3847/1538-4357/ac2154
Billand, J.-B., Elbaz, D., Gentile, F., et al. 2025, , arXiv:2507.04011. doi:10.48550/arXiv.2507.04011
Bolatto, A. D., Levy, R. C., Tarantino, E., et al. 2024, ApJ, 967, 1, 63. doi:10.3847/1538-4357/ad33c8
Briggs, D. S. 1995, Ph.D. Thesis, New Mexico Institute of Mining and Technology.
Burke, C. J., Liu, X., Chen, Y.-C., et al. 2021, MNRAS, 504, 1, 543. doi:10.1093/mnras/stab912
Burke, C. J., Stone, Z., Shen, Y., et al. 2025, , arXiv:2511.16082. doi:10.48550/arXiv.2511.16082
Gaia Collaboration 2020, VizieR Online Data Catalog, 1350. doi:10.26093/cds/vizier.1350
Izotov, Y. I. & Thuan, T. X. 2008, ApJ, 687, 1, 133. doi:10.1086/591660
Latif, M. A., Aftab, A., Whalen, D. J., et al. 2025, A&A, 694, L14. doi:10.1051/0004-6361/202453194
Lin, X., Fan, X., Cai, Z., et al. 2025, , arXiv:2507.10659. doi:10.48550/arXiv.2507.10659
Maiolino, R., Risaliti, G., Signorini, M., et al. 2025, MNRAS, 538, 3, 1921. doi:10.1093/mnras/staf359
Matthee, J., Naidu, R. P., Brammer, G., et al. 2024, ApJ, 963, 2, 129. doi:10.3847/1538-4357/ad2345
Mazzolari, G., Gilli, R., Maiolino, R., et al. 2024, , arXiv:2412.04224. doi:10.48550/arXiv.2412.04224
Pacucci, F., Nguyen, B., Carniani, S., et al. 2023, ApJ, 957, 1, L3. doi:10.3847/2041-8213/ad0158
Perger, K., Fogasy, J., Frey, S., et al. 2025, A&A, 693, L2. doi:10.1051/0004-6361/202452422
Rodríguez, L. F. & Mirabel, I. F. 2025, ApJ, 986, 1, 108. doi:10.3847/1538-4357/adda33
Rose, K., Horesh, A., Murphy, T., et al. 2024, MNRAS, 534, 4, 3853. doi:10.1093/mnras/stae2289
Simmonds, C., Bauer, F. E., Thuan, T. X., et al. 2016, A&A, 596, A64. doi:10.1051/0004-6361/201629310
Soria, R., Russell, T. D., Wiston, E., et al. 2025, PASA, 42, e050. doi:10.1017/pasa.2025.38
Strickland, D. K. 2004, The Interplay Among Black Holes, Stars and ISM in Galactic Nuclei, 222, 249. doi:10.1017/S1743921304002194

Table 1: VLA Observations of J1047+0739

Project	Epoch	Frequency (GHz)	Bandwidth (GHz)	RA(J2000)	DEC(J2000)	Flux Density (μJy)
10B-156	2010 Nov 06	5.0	0.256	10 47 55.899 +/- 0.016	07 39 51.20 +/- 0.12	43 +/- 3
18A-413	2018 Apr 20	6.0	4.0	10 47 55.927 +/- 0.001	07 39 51.26 +/- 0.01	117 +/- 8